Colloid Coalescence with Focused X Rays

B. M. Weon, J. T. Kim, J. H. Je, J. M. Yi, S. Wang, and W.-K. Lee

Phys. Rev. Lett. **107**, 018301 — Published 1 July 2011

DOI: 10.1103/PhysRevLett.107.018301

Colloid Coalescence with Focused X-rays

B. M. Weon,[1,*] J. T. Kim,[1] J. H. Je,[1,†] J. M. Yi,[2] S. Wang,[3] and W.-K. Lee[3]

[1]*X-ray Imaging Center, Department of Materials Science and Engineering, Pohang University of Science and Technology, Pohang, 790-784, Korea*

[2]*Samsung Advanced Institute of Technology, Yongin, Gyeonggi, 446-712, Korea*

[3]*Advanced Photon Source, Argonne National Laboratory, Argonne, Illinois 60439, USA*

ABSTRACT

We show direct evidence that focused X-rays enable to merge polymer colloidal particles at room temperature. This phenomenon is ascribed to photochemical scission of colloids with X-rays, reducing molecular weight, glass transition temperature, surface tension, and viscosity of colloids. The observation of the neck bridge growth with time shows that the X-ray-induced colloid coalescence is analogous to viscoelastic coalescence. This finding suggests a feasible protocol of photonic nanofabrication by sintering or welding of polymers, without thermal damage, using X-ray photonics.

PACS numbers: 47.20.Gv, 82.70.Dd, 81.20.Ev, 87.59.-e

* E-mail: bmweon@hotmail.com, † jhje@postech.ac.kr

Colloidal particles, as one of self-assembling building blocks, are widely studied in an emerging variety of studies and applications [1]. Key examples of colloidal particles are polystyrene (PS) spheres suspended in water and polymethylmethacrylate (PMMA) particles dispersed in hydrocarbon liquids. Coalescence is a fundamental process for merging particles into a solid body [2,3], particularly for novel architectures such as colloidosomes [4] and photonic crystals [5]. The reduction of surface free energy is the driving force for material transport [2,3]. The mechanism of material transport can be elucidated by a direct observation of neck bridge growth between particles [3]. Conventional sintering using heat and/or pressure is often unsuitable to nanoscale colloids due to thermal damage or the difficulty in temperature control [6]. Local rapid heating like laser sintering is an alternative [7]. Laser sintering, however, has risk of thermal damage despite improvements in beam quality, focusing ability, and stability in beam power and position [7].

In this Letter, we present a feasible protocol to merge colloidal particles using X-ray photonics at room temperature. Contrary to laser sintering, X-ray photons can induce photochemical scission without thermal damage [8]. PMMA is a well-known material showing a high yield of chain scission under X-ray irradiation [9]. The scission is mostly due to the loss of ester group ($–CO_2CH_3$) of PMMA [10]. From the studies on various soft matter systems in the past few years [11], we developed a non-thermal ablation technique with X-ray photons via rapid chain scission of polymers [12]. Despite basic knowledge about photochemical scissions of polymers under X-ray irradiation [9,10], a possibility of X-ray-induced coalescence of polymer colloids has been little explored. Here, we present an X-ray-induced coalescence phenomenon of PMMA spheres. The photochemical scission reduces the molecular weight and equivalently the glass transition temperature. The

transition temperature varies with X-ray dose [9]. The reduction of the transition temperature decreases the surface tension and the viscosity, which consequently induces the coalescence process. For both X-ray irradiation and simultaneous imaging, we apply the full-field X-ray transmission microscopy (TXM) at photon energy of 8 keV on the 32-ID imaging beamline of the Advanced Photon Source at the Argonne National Laboratory [13], as illustrated in Fig. 1. This approach is useful not only to directly monitor the coalescence process of colloidal particles in real time, but also to concentrate X-ray photons to induce the coalescence process.

As a model system, we used hard-sphere PMMA colloids with radii of R = 100, 550, 1000, and 1800 nm (polydispersity less than 5%), which were taken from dilute colloidal suspensions of PMMA spheres in decalin [14,15]. The PMMA colloids used here are the spheres (synthesized by A. Schofield) that have a poly(hydroxystearic acid) (PHSA) sterically stabilizing layer 10 nm in thickness. They have been widely used as a model hard-sphere system [1]. The PMMA particles were deposited by evaporation on a clean Kapton tape (Kapton is transparent to X-rays) and directly illuminated with the focused X-rays in a normal direction to the incident X-ray beam. Real-time (Zernike-type) phase-contrast X-ray imaging with a phase ring is performed using the TXM with spatial and temporal resolutions of 40 nm and 50 ms, respectively [13]. The flux of the focused X-ray beam by the condenser lens was $f = 2 \times 10^{11}$ photons s^{-1} at 8 keV [13]. The dose ratio (k) could be estimated as k = 832 photons μm^{-2} Gy^{-1} at 8 keV from the empirical formula [16] of $k = 2000\ \lambda^{-2}$ (where the wavelength is $\lambda = 1.55$ Å at 8 keV). The focused beam size at the sample plane was $15 \times 15\ \mu m^2$ in FWHM (full width at half maximum). Because ~ 95.4% of the incident beam intensity (I) was illuminated to the focal area $A = 25.5 \times 25.5$

μm^2 and the condenser efficiency was $\varepsilon \approx 90\%$, we estimated the dose rate of the focused X-rays as $\mu = 317$ kGy s^{-1} (= 0.954 fεI / kA [16]) on the illuminated sample area. The high dose rate is expected to enhance the X-ray-induced chain scission of PMMA colloids.

Direct visualization of coalescing colloids at the nanoscale is a challenging task [17]. The coalescence process arises from various kinds of mass transports [3] such as evaporation/deposition, surface diffusion, and viscous flow of matter. In the case of a polymer, coalescence is known to occur via "viscous flow" [18,19] or "viscoelastic deformation" [20–22]. The classical Frenkel-Eshelby theory [18,19], equating the rate of work done by surface tension (γ) to the rate of energy dissipation due to viscous flow, predicts that contact radius (r) between two spheres increases with time (t) as $(r/R) \sim (\gamma t/\eta R)^{1/2}$ where R is the radius of coalescing spheres and η is the fluid viscosity. On the other hand, the Johnson-Kendall-Roberts theory [20] predicts "zero slope" for *elastic* coalescence at early stage and also the *viscoelastic* coalescence of $r \sim t^{1/7}$ under zero applied load at late stage [21,22]. Neck bridge measurements, usually observed using optical microscopy with a hot-stage, typically show the *viscous* coalescence for large PS and PMMA spheres (R = 250−300 μm) and the *viscoelastic* coalescence for small spheres (e.g., R ~ 120 μm) [21]. Considering material properties of polymer melts, it has been suggested that colloidal particles from R = 40 nm to R = 2 μm sinter by viscoelastic deformation without any contribution of viscous flow [21]. The most direct approach to verify the coalescence mechanism of colloidal particles at the nanoscale is to simultaneously image the neck growth in real time as the radiation dose is delivered to the sample. Our high-resolution TXM approach can directly visualize the coalescence dynamics of PMMA colloids.

We present representative evidence for the X-ray-induced coalescence of PMMA

colloids with R = 1000 nm at room temperature (20 ^{o}C) in the atmosphere [Fig. 2(a)]. The right area, where PMMA particles are irradiated for 150.1 s by focused X-ray photons, is completely changed into a merged film after the irradiation, clearly showing the X-ray-induced coalescence. Meanwhile the left area irradiated only for 2.6 s (for photography) shows no coalescence. This picture demonstrates the positional selectivity of the coalescence process by locally focusing X-ray photons on the sample. Additional examples for different sized PMMA particles [Fig. 2(b)] show that the coalescence kinetics is likely to become fast as the particle size decreases; as the colloid size decreases from R = 1800 to 100 nm, the complete coalescence time reduces from 198.5 s to 77.3 s. This is attributed to the increase in the surface energy per unit volume with the decrease in the size. The local heating by focused X-rays is negligible, as estimated as $\sim 5 \times 10^{-4}$ K for PMMA [8] under similar irradiation conditions. What causes the coalescence without heating? The answer is the significant reduction of the glass transition temperature of PMMA via photochemical scission by high-flux X-ray bombardment, as is well known [9]. The X-ray dose rate in our case is high as $\mu = 317$ kGy s^{-1} at the focal plane of the sample surface. Such high-flux of X-ray irradiation on a cluster of colloids in contact would possibly reduce the glass transition temperature to room temperature, resulting in the X-ray-induced coalescence without heating.

To illustrate the coalescence dynamics in detail, we take sequential images for PMMA particles with R = 1800 nm [Fig. 3] during the continuous irradiation of X-ray photons. The colloidal particles are gradually merged into a film with the irradiation time. This again confirms that the X-ray irradiation induces the coalescence process of PMMA colloids at room temperature in the atmosphere. The contact radii (r) between colloids are

clearly visible, as illustrated in the photographic image of r ~ 230 nm at the irradiation time of 36.1 s.

We consider possible changes of material properties for the X-ray-irradiated PMMA colloids in terms of glass transition temperature, surface tension, and viscosity, because the photochemical scission reduces the molecular weight. It is well known that the glass transition temperature of PMMA is a function of X-ray dose (μt) as $T_g(t) = T_0 - 0.082 - 9.52$ μt [9] (the coefficient of the last term [9] was adjusted for PMMA) where T_0 is the glass transition temperature of non-irradiated PMMA (= 118.0 ^oC [9]), μ is the dose rate (Gy s^{-1}), and t is the irradiation time (s). Here the $T_g(t)$ of PMMA is not affected by the size for the colloids larger than 100 nm [23,24]. As the X-ray dose increases, the glass transition temperature linearly decreases. We plot $\Delta T = T_0 - T_g(t)$ as a function of the irradiation time [Fig. 4(a)]. After the initial incubation period (~ 30 s), ΔT linearly increases up to 80 K at 60 s. Thus, the glass transition temperature could be reduced to room temperature at 60 s. This explains the room temperature sintering of PMMA colloidal particles by X-ray irradiation.

The reduction of the glass transition temperature would decrease the surface tension and the viscosity of PMMA colloids. The surface tension of PMMA at 20 ^oC is 4.11×10^{-2} N m^{-1} and the temperature dependence is $d\gamma/dT = -7.6 \times 10^{-5}$ N m^{-1} K^{-1} [25]. From $\Delta T = 0.082 + 9.52$ μt, the surface tension is therefore $\gamma(t) = 4.11 \times 10^{-2} - 7.6 \times 10^{-5}$ (0.082 + 9.52 μt). The estimated surface tension [Fig. 4(b)] slightly decreases from 33 N m^{-1} at 32 s to 27 N m^{-1} at 60 s. With the same reason, the viscosity of PMMA particles changes with the glass transition temperature accordingly. To estimate the dependence of the viscosity on ΔT (or the irradiation time), the William-Landel-Ferry equation for PMMA [26] is used as $\eta(t) = \eta_i \exp[-C_1(T - T_i)/(C_2 + (T - T_i))]$ where η_i is the viscosity at a reference temperature T_i.

Here C_1 and C_2 are constants that depend on the reference temperature. We choose the parameters $C_1 = 20.9$ and $C_2 = 58$ for $T < 160$ °C [26]. Taking the glass temperature as the reference temperature, $T - T_i = (\Delta T + 118) - T_i$, we get $\eta_0 = 7.8 \times 10^{10}$ Pa s at $T_i = 105$ °C for a molecular weight (MW) = 10^5 (assuming $\eta \sim MW^{3.4}$) [26]. Based on these parameters, the time-dependent viscosity [Fig. 4(c)] shows a significant decrease of η from ~10^{10} Pa s at 32 s to ~10^5 Pa s at 60 s. Such a remarkable decrease of the viscosity implies that the coalescence takes place by viscoelastic deformation [20–22]. The underlying mechanism of the X-ray-induced coalescence would be analogous to that of thermal sintering in terms of the decrease in the viscosity during the coalescence process.

To clarify the dominant mechanism of the X-ray-induced coalescence, the contact radius growth (the normalized neck radius = r/R) is evaluated as a function of the normalized time (t/τ) as $(r/R) \sim (t/\tau)^{\beta}$ where τ is the viscous time $\tau = (4\pi/3)^{1/3}[\eta(t)R(t)/\gamma(t)]$ [Fig. 4(d)] [21]. In the log-log plot of (r/R) versus (t/τ), the slope β informs possible coalescence mechanisms [3,21,22]. Our measurement from 7 particles [Fig. 3] shows a significant slope transition after $t/\tau > 0.04$ and indeed gives the slope β around 1/6 (between 1/5 and 1/7, if we include the error bars [one standard deviation]) [Fig. 4(d)]. The 1/7 or 1/5 scaling is consistent with the theoretical prediction based on the viscoelastic coalescence [22]. We conclude that the early behavior comes from the elastic contact behavior (the slope ~ 0) [22] and the late behavior from the viscoelastic coalescence (the slope ~ 1/6), as expected for typical polymer sintering [21,22].

In principle, Van der Waals and Young-Laplace forces can contribute to polymer coalescence [22] in three successive steps: (i) elastic adhesive contact, (ii) “zipping” contact growth driven by adhesive forces and accommodated by viscoelastic deformation, and (iii)

"stretching" contact growth driven by the surface tension and accommodated by viscous flow. Recent simulation results [21] showed that the traditional viscous coalescence model (by capillary forces) holds for large particle size (> 10 μm) and a significant deviation must exist for small colloidal particles (< 10 μm) of identical materials. They predicted that the effect of van der Waals forces would become dominant for small sizes [21]. Our result shows evidence that the $t^{1/5}$ or $t^{1/7}$ scaling indeed appears in the coalescence kinetics of colloidal dimensions, suggesting the dominance of van der Waals forces.

Is there another possible mechanism for the colloidal particle coalescence? One possibility is the surface diffusion, typically observed with a scaling ($r \sim t^{1/7}$) in the coalescence of heated metal particles [27]. However, this is not probable since the surface diffusion rate of colloidal particles would be too slow to induce coalescence; e.g., it would take 1 year for a surface molecule to diffuse to the other side of a 10 μm particle, because the time is proportional to the mean-square diffusion distance [28]. Our observation of neck growth of $t^{1/6}$ suggests that colloid coalescence by X-ray irradiation is analogous to viscoelastic coalescence ($t^{1/5}$ or $t^{1/7}$) [20–22], instead of viscous ($r \sim t^{1/2}$) [18,19] or diffusive coalescence ($r \sim t^{1/7}$) [27]. Importantly, colloid coalescence differs from liquid coalescence in terms of capillary speed (γ/η) [29,30]: $\gamma/\eta < 10^{-7}$ m s^{-1} for colloids [Fig. 4] is much smaller than that for ordinary liquids (e.g., ~ 70 m s^{-1} for water). Viscoelastic deformation controls colloid coalescence, whereas capillary speed controls liquid coalescence.

In conclusion, we present a direct observation of an X-ray-induced coalescence in polymer colloids. We observe nanoscale coalescence phenomena of colloids in real time with the full-field X-ray transmission microscopy (TXM). The key mechanism of the non-thermal sintering is the X-ray-induced photochemical scission reducing the molecular

weight, which effectively diminishes the glass temperature, the surface tension, and the viscosity of PMMA particles. High resolution imaging from the TXM offers direct evidence that contact neck grows with time initially by zero slope and in turn by 1/6 power-law scaling. This result well agrees with a typical transition of polymer sintering from elastic coalescence at early stage to viscoelastic coalescence at late stage. Conventional sintering using heat and/or pressure would be unsuitable to nanoscale colloids because of thermal damage. X-ray photons can effectively induce coalescence via photochemical scission without thermal damage in nanoscale spatial resolution. Our findings can open opportunities of sintering or welding technology for polymers by modifying their structures and properties using X-ray photonics, which can be applied either at laboratory sources or at synchrotron radiation sources. The X-ray-induced coalescence may be meanwhile a very critical problem in probing colloidal or nanoparticle samples by high-brilliance X-ray sources.

Acknowledgements

This work was supported by the Creative Research Initiatives (Functional X-ray Imaging) by MEST/NRF. Use of the Advanced Photon Source at Argonne National Laboratory was supported by the U. S. Department of Energy, Office of Science, Office of Basic Energy Sciences, under Contract No. DE-AC02-06CH11357.

References

[1] P. N. Pusey and W. van Megen, Nature (London) **320**, 340 (1986).

[2] M. Bowker, Nature Mater. **1**, 205 (2002).

[3] W. D. Kingery and M. Berg, J. Appl. Phys. **26**, 1205 (1955).

[4] A. D. Dinsmore *et al.*, Science **298**, 1006 (2002).

[5] A. van Blaaderen *et al.*, Nature (London) **385**, 321 (1997).

[6] D. Wakuda *et al.*, Chem. Phys. Lett. **441**, 305 (2007).

[7] C. M. Stotko, Nature Photonics **3**, 265 (2009).

[8] J. Wang *et al.*, J. Synchrotron Radiat. **14**, 181 (2007).

[9] H. R. Keymeulen *et al.*, J. Appl. Phys. **102**, 013528 (2007).

[10] J. Wang *et al.*, J. Electron Spectrosc. Relat. Phenom. **170**, 25 (2009).

[11] B. M. Weon *et al.*, Phys. Rev. Lett. **100**, 217403 (2008); B. M. Weon *et al.*, J. Synchrotron Radiat. **15**, 660 (2008); B. M. Weon and J. H. Je, Appl. Phys. Lett. **93**, 244105 (2008).

[12] B. M. Weon *et al.*, J. Appl. Phys. **106**, 053518 (2009); B. M. Weon *et al.*, ChemPhysChem **11**, 115 (2010).

[13] Y. S. Chu *et al.*, Appl. Phys. Lett. **92**, 103119 (2008).

[14] L. Xu *et al.*, Phys. Rev. Lett. **101**, 094502 (2008).

[15] B. M. Weon and J. H. Je, Phys. Rev. E **82**, 015305 (2010).

[16] J. M. Holton, J. Synchrotron Radiat. **16**, 133 (2009).

[17] M. A. Asoro *et al.*, Nanotechnology **21**, 025701 (2010).

[18] J. Frenkel, J. Phys. (Moscow) **9**, 385 (1945).

[19] J. D. Eshelby, Metals Trans. **185**, 806 (1949).

[20] K. L. Johnson *et al.*, Proc. R. Soc. Lon. A **324**, 301 (1971).

[21] A. Jagota *et al.*, J. Appl. Phys. **83**, 250 (1998).

[22] Y. Y. Lin *et al.*, J. Colloid Interf. Sci. **237**, 267 (2001).

[23] J. L. Keddie, R. A. L. Jones, and R. A. Cory, Europhys. Lett. **27**, 59 (1994).

[24] M. Alcoutlabi and G. B. McKenna, J. Phys: Condens. Matter **17**, R461 (2005).

[25] L. Rontzsch *et al.*, Appl. Phys. Lett. **90**, 044105 (2007).

[26] C. Carelli *et al.*, Phys. Rev. E **73**, 061804 (2006).

[27] J. Eggers, Phys. Rev. Lett. **80**, 2634 (1998).

[28] Y. Min *et al.*, Nature Mater. **7**, 527 (2008).

[29] J. D. Paulsen, J. C. Burton, and S. R. Nagel, Phys. Rev. Lett. **106**, 114501 (2011).

[30] J. S. Lee *et al.*, Nature Commun. (2011), DOI: 10.1038/ncomms1369.

Figure Captions

FIG. 1: (Color online) Schematic illustration of the X-ray-induced coalescence of polymer colloids. (a) Full-field X-ray transmission microscopy (TXM) setup: X-ray photons are focused on the sample via the capillary condenser lens and gathered through the zone plate objective on the CCD camera. (b) The coalescence process (necking) between colloids is induced by the focused X-rays.

FIG. 2: (Color online) (a) Evidence of coalescence for PMMA colloids (R = 1000 nm) with the focused X-rays (8 keV). This image was taken using the TXM during X-ray irradiation. The long-irradiated area (right), which was fully merged for 150.1 s, shows the X-ray-induced coalescence, while the short-irradiated area (left) for 2.6 s (for photography) shows no coalescence. (b) Additional examples for different sized PMMA particles. The coalescence kinetics becomes fast as the particle size decreases.

FIG. 3: (Color online) Monitoring of a single coalescence event for PMMA colloids (R = 1800 nm) with the focused X-rays (8 keV). Sequential images taken using the TXM show that the colloidal particles are gradually merged into a film with irradiation time. Schematic (down left) shows the X-ray-induced coalescence process. The contact radii between colloids (down right) are visible as r ~ 230 nm at 36.1 s.

FIG. 4: (Color online) Changes of material properties of PMMA with X-rays. (a) The change of the glass transition temperature is described as $\Delta T = T_0 - T_g(t)$ for T_0 $[T_g(t)]$

without [with] irradiation. After initial incubation time (~ 30 s), ΔT linearly increases with irradiation time, implying a significant reduction of $T_g(t)$ to room temperature at 60 s. (b) Surface tension (γ) slightly decreases with irradiation time. (c) Viscosity (η) significantly decreases with irradiation time. (d) Normalized contact radius (r/R) versus normalized coalescence time (t/τ) demonstrates that the 1/6 slope (solid line) emerges at late stage, implying the viscoelastic coalescence.

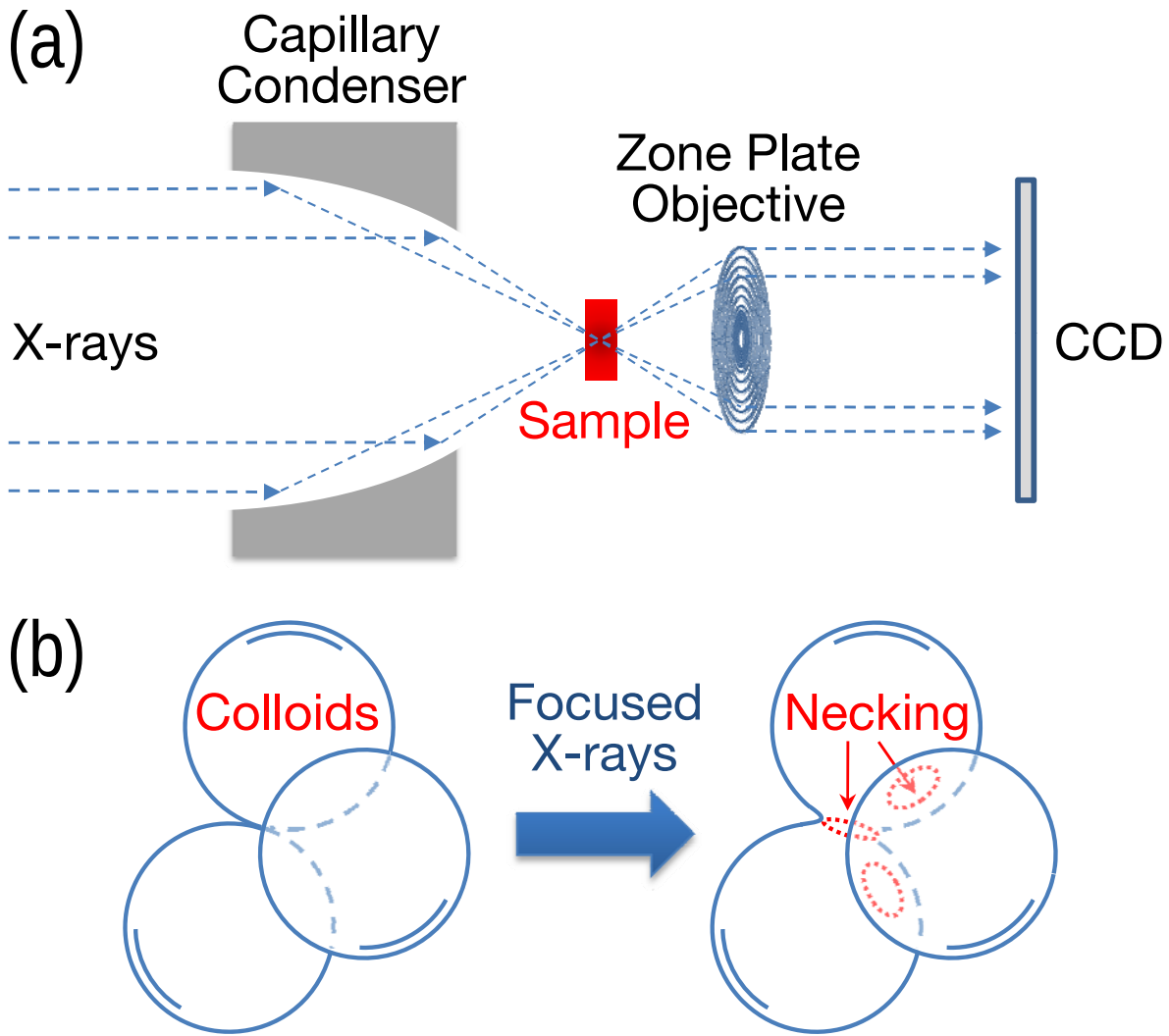
(a)
Capillary
Condenser
Zone Plate
Objective
X-rays
Sample
CCD
(b)
Colloids
Focused
X-rays
Necking

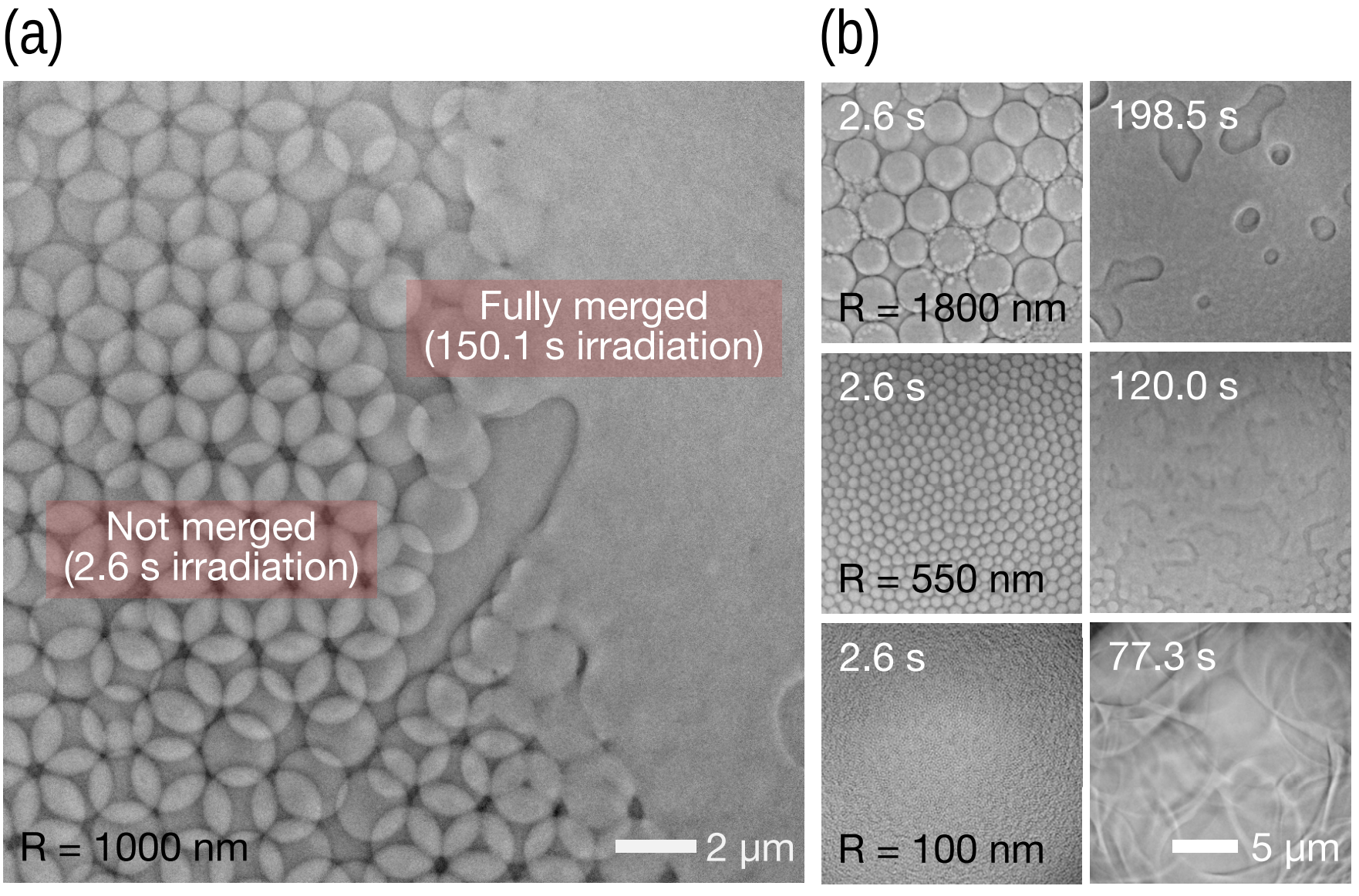
(a)
Fully merged
(150.1 s irradiation)
Not merged
(2.6 s irradiation)
R = 1000 nm
2 μm
(b)
2.6 s
R = 1800 nm
198.5 s
2.6 s
R = 550 nm
120.0 s
2.6 s
R = 100 nm
77.3 s
5 μm

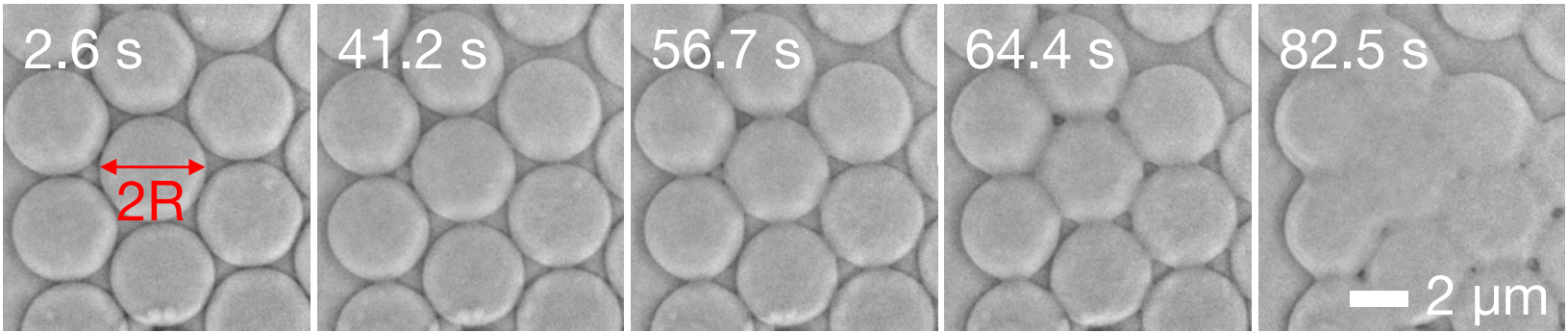
2.6 s
2R
41.2 s
56.7 s
64.4 s
82.5 s
2 μm

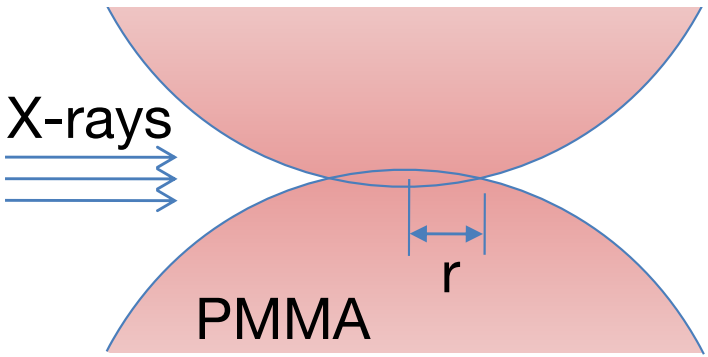
X-rays
r
PMMA

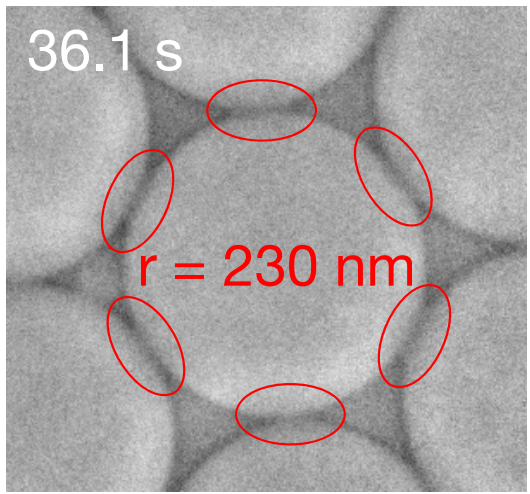
36.1 s
r = 230 nm

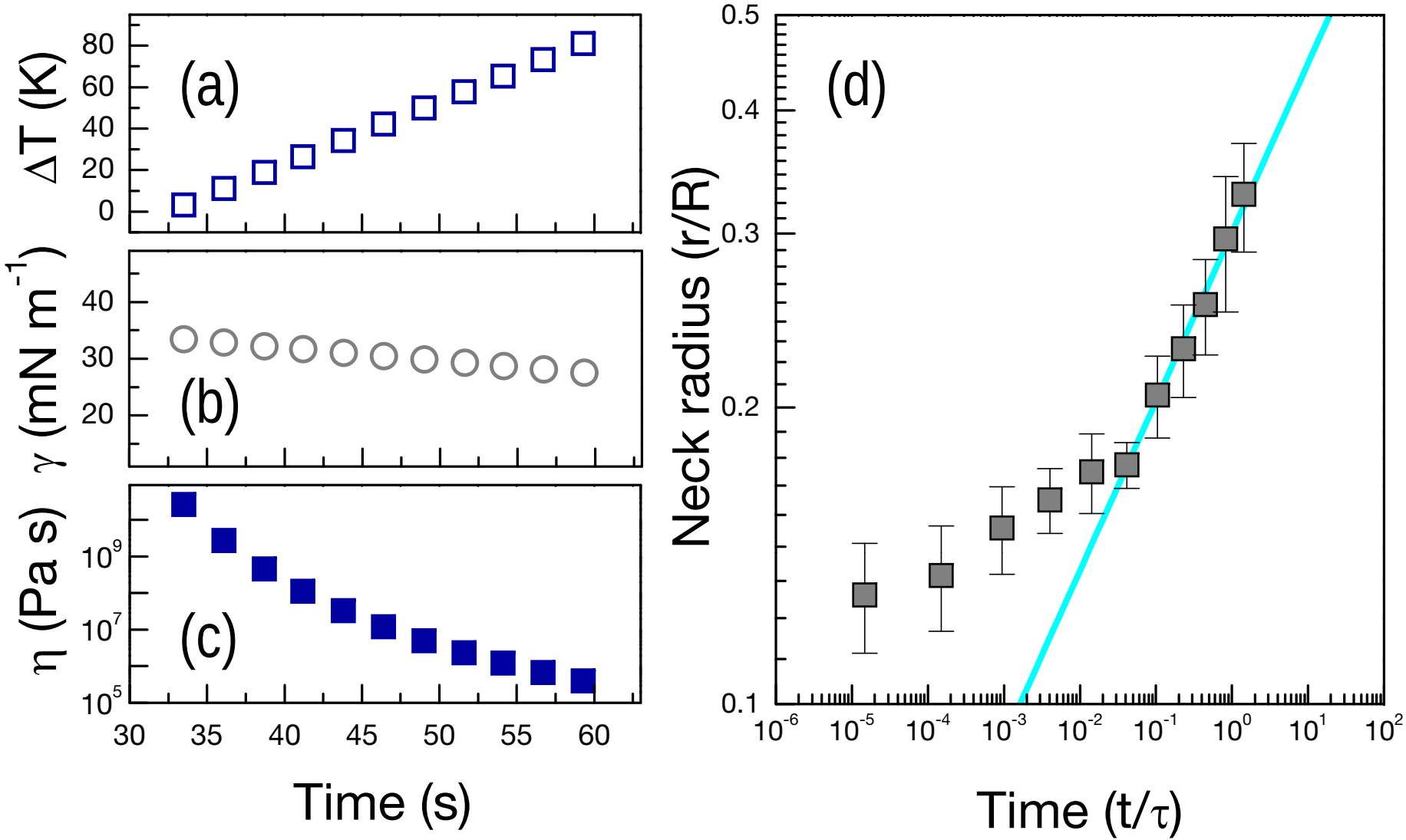
(a)
ΔT (K)
80
60
40
20
0
(b)
γ (mN m-1)
40
30
20
(c)
η (Pa s)
10^9
10^7
10^5
30
35
40
45
50
55
60
Time (s)
(d)
Neck radius (r/R)
0.5
0.4
0.3
0.2
0.1
10^-6
10^-5
10^-4
10^-3
10^-2
10^-1
10^0
10^1
10^2
Time (t/τ)